Water Resources Research

RESEARCH ARTICLE
10.1029/2018WR023024

Application of the Beer–Lambert Model to Attenuation of Photosynthetically Active Radiation in a Shallow, Eutrophic Lake

Chelsea J. Weiskerger[1], Mark D. Rowe[2], Craig A. Stow[3], Dack Stuart[2], and Tom Johengen[2]

[1]Civil and Environmental Engineering, Michigan State University, East Lansing, MI, USA, [2]Cooperative Institute for Great Lakes Research, University of Michigan, Ann Arbor, MI, USA, [3]NOAA Great Lakes Environmental Research Laboratory, Ann Arbor, MI, USA

Key Points:
- The Beer–Lambert law effectively models photosynthetically active radiation in western Lake Erie, despite some systematic deviations
- Field-obtained water quality parameters can predict photosynthetically active radiation attenuation with a high degree of confidence
- Suspended particle concentration is most predictive of photosynthetically active radiation attenuation in this turbid, eutrophic basin

Supporting Information:
- Supporting Information S1
- Data Set S1

Correspondence to:
C. J. Weiskerger,
weiskerg@egr.msu.edu

Citation:
Weiskerger, C. J., Rowe, M. D., Stow, C. A., Stuart, D., & Johengen, T. (2018). Application of the Beer–Lambert model to attenuation of photosynthetically active radiation in a shallow, eutrophic lake. *Water Resources Research*, *54*, 8952–8962. https://doi.org/10.1029/2018WR023024

Received 28 MAR 2018
Accepted 15 OCT 2018
Accepted article online 22 OCT 2018
Published online 14 NOV 2018

Abstract Models of primary production in aquatic systems must include a means to estimate subsurface light. Such models often use the Beer–Lambert law, assuming exponential attenuation of light with depth. It is further assumed that the diffuse attenuation coefficient may be estimated as a summation of scattering/absorbing constituent concentrations multiplied by their respective specific attenuation coefficients. While theoretical deviations from these assumptions have been documented, it is useful to consider the empirical performance of this common approach. Photosynthetically active radiation (PAR) levels and water quality conditions were recorded weekly from six to eight monitoring stations in western Lake Erie between 2012 and 2016. Exponential PAR extinction models yielded a mean attenuation coefficient of 1.55 m (interquartile range = 0.74–1.90 m). While more complex light attenuation models are available, analysis of residuals indicated that the simple Beer–Lambert model is adequate for shallow, eutrophic waters similar to western Lake Erie ($R^2 > 0.9$ for 96% of samples). Three groups of water quality variables were predictive of PAR attenuation: total and nonvolatile suspended particles, dissolved organic substances (dissolved organic carbon and chromophoric dissolved organic matter), and organic solids (volatile suspended solids and chlorophyll). Multiple regression models using these variables predicted 3–90% of the variability in PAR attenuation, with a median adjusted $R^2 = 0.86$. Explanatory variables within these groups may substitute for each other while maintaining similar model performance, indicating that various combinations of water quality variables may be useful to predict PAR attenuation, depending on availability within a model framework or monitoring program.

1. Introduction

Light penetration plays a critical a role in aquatic ecology, regulating phytoplankton and submerged aquatic vegetation growth, organic carbon production, hypoxia prevention, and the ability of visual predators to find prey (Karlsson et al., 2009; Kemp et al., 2005). Cyanobacterial buoyancy has been modeled as a function of light exposure (Medrano et al., 2013), as have the fate and transport of bacteria (Ge et al., 2012; Safaie et al., 2016). Physically, light penetration contributes to water column warming and stratification (Hondzo & Stefan, 1993; Houser, 2006). Therefore, light attenuation is an important component of many mechanistic freshwater and marine system models (Chen et al., 2003; Ji et al., 2008; Rowe et al., 2017). A light attenuation coefficient is often specified as a function of water quality constituent concentrations within such models (Christian & Sheng, 2003; Dennison et al., 1993; Stefan et al., 1983; Xu et al., 2005).

Light attenuation models range from simple to complex, and various approaches may be appropriate depending on the system being modeled and the model objective. Light attenuation differs by wavelength, water column depth, and concentration of absorbing or scattering constituents (Markager & Vincent, 2000; Smith, 1982; Stefan et al., 1983). In the visible spectrum, long and short wavelengths (red and violet) are absorbed or scattered over a relatively short distance, while intermediate wavelengths (green) penetrate most deeply (Gordon & McCluney, 1975; Hutchinson & Edmondson, 1957; Jerlov, 1968). In addition to absorption and scattering by the water itself, particles can scatter light with wavelengths 0 to 4 times the particle diameter (Ensor & Pilat, 1971). When modeling phytoplankton growth or primary production is the goal, as is common for eutrophic waters, a useful simplification is to aggregate across the wavelengths of

photosynthetically active radiation (PAR; 400–700 nm (Kirk, 1983; Xu et al., 2005)). A further simplification is to apply the Beer–Lambert law, in which exponential attenuation of light with depth is assumed (Hutchinson & Edmondson, 1957; Ingle & Crouch, 1988). It is further assumed that the diffuse attenuation coefficient may be estimated as a summation of concentrations of scattering/absorbing constituents multiplied by their respective specific attenuation coefficients. While theoretical deviations from these assumptions have been documented (Gordon, 1989; Stavn, 1988), it is useful to consider the empirical performance of this approach, given its wide application in mechanistic models of aquatic systems (Bocaniov et al., 2016; Cerco & Meyers, 2000; Ji et al., 2008; Rowe et al., 2017; Verhamme et al., 2016). In a purely physical model, water quality constituent concentrations may not be available as model state variables, while biophysical models differ greatly in the state variables that are included.

Similarly, monitoring programs differ in the water quality and physical variables that are measured. Thus, it is useful to determine the best water quality and physical variable predictors of light attenuation, and also to consider the general applicability of the models, in terms of ability to substitute variables without losing predictive ability.

Because of its widely varying light attenuation and water quality conditions, western Lake Erie provides an ideal location to develop PAR attenuation models that may be representative of shallow, turbid, and productive systems. Western Lake Erie is a large, shallow, eutrophic, freshwater system, which exhibits heterogeneous water quality conditions due to mixing of waters from the Detroit and Maumee Rivers, and wave-generated sediment resuspension. A cyanobacterial bloom consisting mainly of *Microcystis aeruginosa* has occurred to a varying extent each summer for the past 15 years (Stumpf et al., 2012). Western Lake Erie is too shallow to seasonally stratify (Chandler, 1942; Mortimer, 1987); thus, water quality variables are often vertically uniform. However, under calm conditions, buoyant *Microcystis* colonies often concentrate near the surface (Rowe et al., 2016).

We aimed to characterize PAR attenuation in western Lake Erie and to determine whether the Beer–Lambert model, which is commonly used within mechanistic biophysical models, adequately describes the attenuation of PAR within the water column. We further determined the dependence of PAR attenuation on water quality constituents. Given that mechanistic biophysical models differ in terms of the water quality variables that are represented, we wanted to evaluate combinations of predictors, and determine the most parsimonious models without sacrificing prediction of the diffuse attenuation coefficient for PAR ($k_{d(\mathrm{PAR})}$). Though these types of models have been developed for Lake Erie and other surface waters in the past (McMahon et al., 1992; Saulquin et al., 2013; Smith, 1982; Stefan et al., 1983), the lake system is constantly changing as a result of invasive species, changes to tributary inputs and nutrient/contaminant loading associated with sediment resuspension (Porta et al., 2005). Especially when mechanistic biophysical models rely on light attenuation estimates to predict primary productivity and biological conditions, periodic reevaluation of existing models is necessary.

2. Materials and Methods

2.1. Field Data Collection

Vertical profiles of PAR were collected using a Sea-Bird Electronics (SBE) 19plus SeaCAT Profiler Conductivity, Temperature, Depth instrument (referred to hereafter as "CTD") and a Biospherical PAR sensor (model QSP 2300). Profiles were collected weekly between June and November of 2012–2016, at six to eight stations in the western basin of Lake Erie (Figure 1). The CTD had a 4-Hz sampling rate for measuring conductivity, temperature, water pressure (depth), and PAR. The PAR sensor was located 0.435 m above the CTD pressure sensor, and all readings were depth-corrected accordingly. Additional water quality data were obtained from grab samples collected concurrently with PAR profiles at approximately 0.5 m below the surface. Samples were analyzed for total suspended solids (TSS; mg/L), volatile suspended solids (VSS; mg/L), dissolved organic carbon (DOC; mg/L); chromophoric-dissolved organic matter (CDOM; absorption at 400 nm, m), and chlorophyll *a* (CHL; μg/L). TSS was measured gravimetrically after filtering samples through a predried, preweighed Whatman GFC 47-mm filter. The filter was then combusted for 4 hr at 450 °C, cooled, and reweighed to measure VSS (APHA, 1998). For DOC measurement, U.S. EPA method 415.3 (USEPA, 2005) was followed, while CDOM was measured using absorbance at 400 nm instead of 254 nm, following Mitchell et al. (2003) and Mouw and Barnett (2014). Chlorophyll concentrations were determined by filtering 100 mL of sample through a 45-mm Whatman GF/F filter under low vacuum pressure. After filtration, filters were frozen in

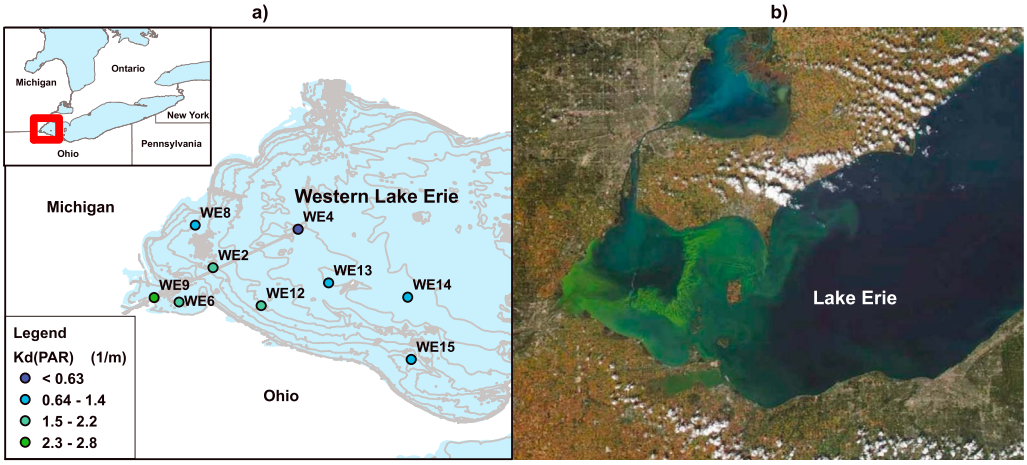

Figure 1. (a) Map of the western Lake Erie study area and weekly monitoring stations, showing mean $k_{d(PAR)}$ by station from this study, 1-m bathymetry contours, and (b) satellite image showing typical spatial variation in water quality during summer in western Lake Erie (NASA MODIS imagery and NOAA CoastWatch, taken 30 September 2014).

polypropylene tubes until extraction. Chlorophyll *a* was extracted from the filtered material using N,N-dimethylformamide (DMF; Speziale et al., 1984). DMF was added to the tubes and heated in a water bath at 65 °C for 15 min. After agitation and centrifugation, the supernatant was analyzed on a Turner Design 10-AU fluorometer for Chl *a* using nonacidification. In addition to water quality variables, hourly wind speed was interpolated from stations surrounding Lake Erie, according to methods developed for NOAA GLERL's Great Lakes Coastal Forecasting System (Beletsky et al., 2003).

2.2. Estimating $k_{d(PAR)}$

We used vertical PAR radiation (μmol m^{-2} s^{-1}) profiles (Figure 2) to estimate the diffuse light attenuation coefficient, $k_{d(PAR)}$, by fitting the Beer–Lambert law for the exponential extinction of light in water (equation (1); Ingle & Crouch, 1988). Using the Beer–Lambert law,

$$\ln(I_z) = \ln(I_0) - k_{d(PAR)}z \tag{1}$$

$k_{d(PAR)}$ and surface PAR, I_0, were estimated for each CTD cast by linear least squares regression of ln (I_z) versus depth, where I_z represents subsurface PAR at depth z. Because I_0 is obtained from regression, rather than being measured independently, this parameter represents PAR just below the surface, and surface

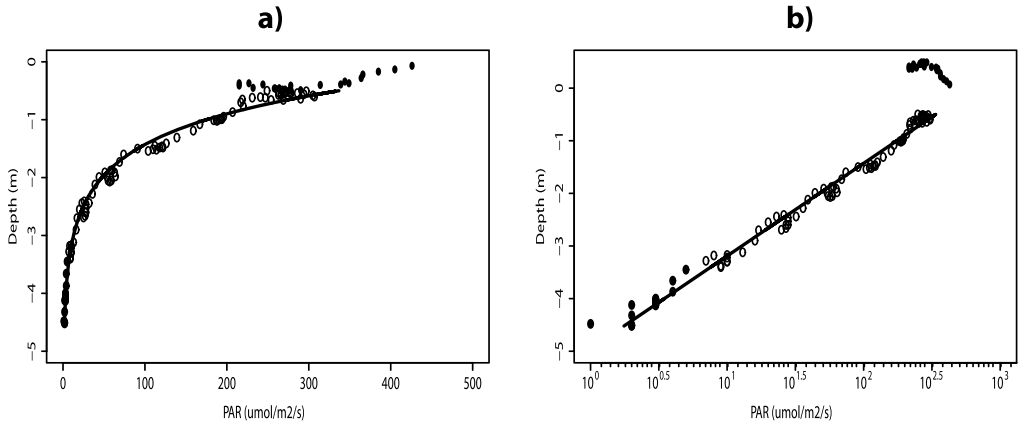

Figure 2. (a) Example raw and (b) semilog format vertical profiles of PAR in western Lake Erie (circles) and the fitted Beer–Lambert law (line). Filled circles represent data from the CTD cast that were either collected at <5-m depth or at depth exceeding the euphotic zone, and thus were not used in further analysis.

phenomena such as reflection or absorption by surface scums would need to be treated separately in order to calculate subsurface PAR from incident PAR using the values of $k_{d(\mathrm{PAR})}$ estimated in this study.

We used an iterative process to determine both the depth of the euphotic zone and the resulting $k_{d(\mathrm{PAR})}$ coefficient representative of the euphotic zone. The initial iteration calculated the depth of the euphotic zone, defined as the depth to reach 1% of surface PAR radiation, I_0. Values associated with depths beyond the euphotic zone as well as depths less than 0.5 m were removed from profile data, and the Beer–Lambert law was fit over the remaining euphotic zone PAR values in the second iteration. PAR data collected at depths shallower than 0.5 m were ignored because the PAR sensor could not be fully submerged at such depths.

2.3. Statistical Models for Predicting $k_{d(\mathrm{PAR})}$

Multiple regression models were developed to predict the estimated $k_{d(\mathrm{PAR})}$ as a function of water quality or physical variables. For quality assurance, we limited our regression analyses to $k_{d(\mathrm{PAR})}$ estimates whose Beer–Lambert models fit with R^2 values greater than 0.9 (197 records; Table S1). Model performance was ranked using multiple metrics. Spearman correlation and regression tree analysis were used to identify candidate predictor variables that were most associated with $k_{d(\mathrm{PAR})}$. Regression tree analysis was used to rank the relative influence of multiple predictor variables, allowing for nonlinear relationships and interactions by partitioning the data into a series of significantly different ($\alpha = 0.05$) groups of at least 10 observations. Relative model performance was screened using stepwise linear regression analysis of variable combinations.

Variables representing the same group (total or nonvolatile suspended particles, organic particles, dissolved organic substances) were not combined, to minimize problems arising from multicollinearity. Models that minimized the Akaike information criterion (AIC) were considered to be higher-performing, considering predictive ability within the training data as well as parsimony. We evaluated predictive skill of the models outside of the training data using a 10-fold cross-validation method; the data were randomly split into 10 groups, a model was fit using nine groups, and residuals were calculated using the one group that was left out of the initial fit. The cross-validation process was repeated until residuals were calculated on each of the 10 groups, and then root-mean-square error (RMSE) was calculated from the residuals.

3. Results

The Beer–Lambert law approximated PAR attenuation well, with 96% of profile models (691 out of 719) yielding R^2 values >0.90. Despite these high R^2 values, residuals plots of the Beer–Lambert models occasionally showed systematic variation (Figure 3), indicating that the models may not have captured all of the variability in the data. The standardized residuals accumulated over all Beer–Lambert models indicated underprediction of PAR at shallow and deep extremes, and overprediction of PAR levels at moderate depths in the casts (Figure 3a). This trend is also manifest in a typical residual plot for the Beer–Lambert approximation (Figure 3b).

The six selected water quality predictor variables represented three major groups: total or nonvolatile particles, dissolved organic matter, and organic particles (Table 1). In most cases, VSS constituted a much smaller proportion of TSS than nonvolatile suspended solids (NVSS), leading to greater correlations between TSS and NVSS than between TSS and VSS. Additional potential predictors included total phosphorus, particulate organic nitrogen, and particulate organic carbon. These additional variables were not found to be as highly correlated with PAR and $k_{d(\mathrm{PAR})}$ as TSS, VSS, NVSS, DOC, CDOM, and CHL, and were therefore removed from further analysis. The pairs of variables within each of the three main groups (total and nonvolatile suspended particles, dissolved organic matter, and organic particles) were highly correlated with one another (Figure 4). This supported the conceptual basis for the groups of variables; these pairs indicated similar influences on $k_{d(\mathrm{PAR})}$, and that predictors may substitute for one another in statistical models.

Water quality parameters in western Lake Erie exhibited a wide range of values. Relative standard deviations for suspended solids and chlorophyll concentrations were greater than for dissolved organic matter, with values of 134%, 119%, and 36% for NVSS, CHL, and DOC, respectively (Figure 5).

Single variable regression models and Spearman rank correlations indicated which individual water quality variables were most predictive of $k_{d(\mathrm{PAR})}$ (Table 2). Water quality variables that gave Spearman rank correlation coefficients, ρ, discernible from zero included TSS, NVSS, DOC, and CDOM. TSS and NVSS were most

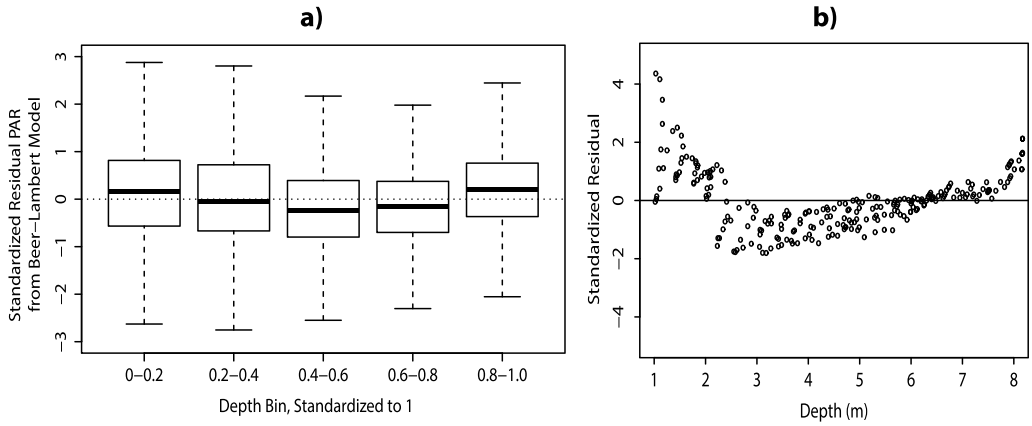

Figure 3. (a) Standardized residual plots for Beer–Lambert approximations of PAR attenuation with depth, summarized for all CTD casts in boxplot form and (b) showing a typical residual pattern observed for an individual cast. In (a), depths were standardized to 1, with each bin representing 20% of the euphotic zone depth.

highly correlated with $k_{d(\mathrm{PAR})}$ (Spearman's $\rho = 0.85$ and 0.83, respectively), while CHL and VSS showed much lower correlation coefficients ($\rho = 0.38$ and 0.51, respectively). DOC and CDOM showed intermediate correlation coefficients ($\rho = 0.62$ and 0.60, respectively). Single-variable linear regression analyses resulted in a similar ranking. Regression analyses of $k_{d(\mathrm{PAR})}$ on TSS and NVSS yielded R^2 values of 0.85 and 0.81, respectively. VSS and CHL were less predictive of $k_{d(\mathrm{PAR})}$, yielding R^2 values of 0.09 and 0.03, respectively (Table 2). Regression tree analysis also identified TSS and NVSS as the most important contributors to $k_{d(\mathrm{PAR})}$ (Figure 6). The combination of TSS, NVSS, and CDOM explained 80.3% of the total variability in $k_{d(\mathrm{PAR})}$, with high levels of total suspended solids leading to the highest $k_{d(\mathrm{PAR})}$ values.

Combining water quality variables into multiple regression models led to higher predictive ability than the use of single-variable models or regression trees. After 10-fold cross-validation, nine models were identified that gave similarly high adjusted R^2 values (ranging from 0.87 to 0.90), and at the same time gave the lowest RMSE values of the candidate models (from 0.42 to 0.45 m; Figure 7 and Table S2), indicating their predictive ability outside of the training data.

The model that maximized adjusted R^2 while minimizing RMSE, AIC score, and RSS value included NVSS, DOC, and CHL concentrations (AIC = −342.02, RSS = 33.33; Table S2 and equation (2)).

$$K_{d(PAR)} = 0.083(NVSS) + 0.184(DOC) + 0.005(CHL) - 0.096 + \varepsilon \quad (2)$$

Despite the high R^2 values of these models, they tend to capture less of the variance in the data at extreme $k_{d(\mathrm{PAR})}$ values than near the median (Figure 8). The optimized models overpredict at low $k_{d(\mathrm{PAR})}$ and underpredict at high $k_{d(\mathrm{PAR})}$ values. Model residuals (Figure 8a) indicate that variance increases with PAR attenuation coefficient value, and this change in variability is not fully captured by the models.

We also investigated physical variables as candidate predictors for $k_{d(\mathrm{PAR})}$. Water depth and $k_{d(\mathrm{PAR})}$ were significantly correlated ($\rho = -0.52$, $p < 0.01$), while time-averaged wind speed values were less correlated with $k_{d(\mathrm{PAR})}$. The Spearman's ρ correlation coefficient between $k_{d(\mathrm{PAR})}$ and wind speed averaged over a range of preceding time intervals was maximized for 120-hr (five-day) averaged wind speed ($\rho = 0.130$, $p < 0.01$; Figure 9). The lowest-magnitude correlation coefficients were observed for wind speeds averaged over 4 and 312 hr prior to the PAR attenuation observations ($\rho < 0.01$ and 0.01, $p = 0.51$ and 0.42, respectively).

Multiple regression models incorporating water depth and wind speed were not as effective as water quality parameters at predicting $k_{d(\mathrm{PAR})}$, with adjusted R^2 values ranging from 0.284 to 0.310. Corresponding RMSE values were relatively high, ranging from 0.764 to 0.781 m (Table S3).

Table 1
Water Quality Variables Used as Predictors of PAR Attenuation in Western Lake Erie, 2012–2016

Water Quality Predictor Variable	Variable Group
TSS	Total or nonvolatile particles
VSS	Organic particles
NVSS	Total or nonvolatile particles
CDOM	Dissolved organic matter
DOC	Dissolved organic matter
CHL	Organic particles

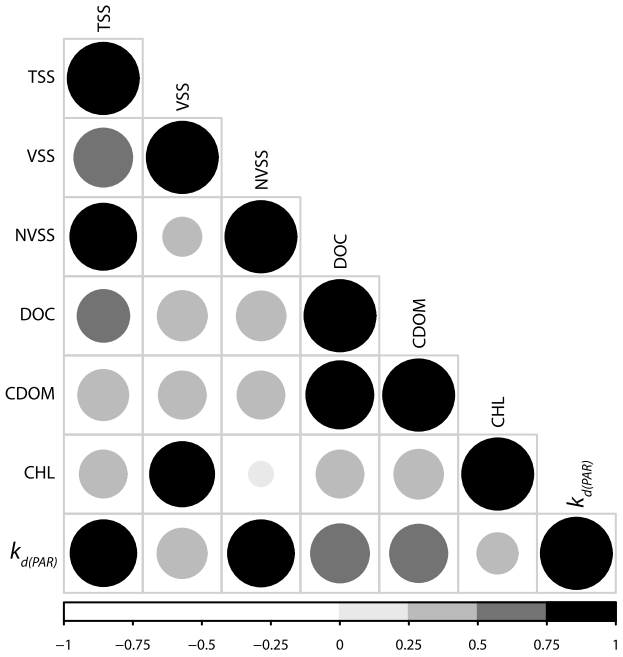

Figure 4. Correlation matrix for water quality variables and $k_{d(PAR)}$. Circle size and color represent the magnitude of the correlation coefficient between the variables.

4. Discussion

Models using TSS, VSS, NVSS, DOC, CDOM, and CHL as predictor variables effectively captured up to 90% of the variation in PAR attenuation coefficients for the western basin of Lake Erie. Models using different combinations of variables representing total and nonvolatile particles, organic particles, and dissolved organic matter showed similar skill, providing a means to estimate $k_{d(PAR)}$ that would be suitable for use within more complex mechanistic models in which the availability of specific water quality variables may depend on the model framework.

Beer–Lambert approximations of PAR attenuation (equation (1)) were highly predictive, with R^2 values above 0.90 in the majority of cases. However, residual plots compiled over all profiles showed a systematic deviation. This suggests that there is autocorrelation in the data that may be better captured by more complex models. Some wavelengths of light attenuate faster than others, leading to greater curvature in the PAR profile than can be accommodated by equation (1). Alternative forms of the Beer–Lambert law are available, for example, those that combine two exponential terms to accommodate faster and more slowly attenuating wavelengths. For example, Paulson and Simpson (1977) found that the transition between the faster and slower attenuation rate occurred between ~5- and 10-m depth in type I, II, and III waters. In our data, depth was $<$10 m, so most of our euphotic zone depths would have captured only the shallower end of this transition zone, which is typical of turbid coastal waters. For more transparent waters, a double-exponential or mixed model (Borsuk & Stow, 2000) may be more appropriate. In our case, despite some indication of systematic deviation in residuals plots, the majority of standardized residuals were small in magnitude, relative to the PAR values that were modeled (Figure 3), suggesting that overall fits to the data were acceptable for our purposes. Therefore, these models can effectively predict PAR attenuation in western Lake Erie for use in mechanistic primary production, water quality, and hydrodynamic modeling frameworks that require estimates of subsurface PAR.

PAR attenuation coefficients for western Lake Erie between 2012 and 2016 ranged from 0.12 to 9.08 m, with an average value of 1.67 ± 1.30 m. These attenuation values are twice as high as those observed by Fitzpatrick et al. (2007) and Dahl et al. (1995) for the northern and central regions of western Lake Erie, but are closer to $k_{d(PAR)}$ results from 1997 samples taken throughout the western basin (Smith et al., 2005). These differences may be associated with differences in sampling locations for each respective study within the basin. This is

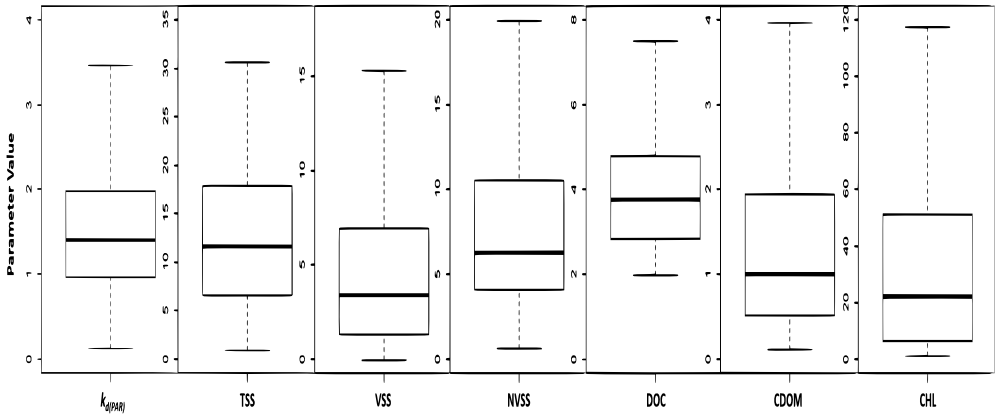

Figure 5. Boxplots showing the range of values of $k_{d(PAR)}$ and predictor variables used in multiple regression models for PAR attenuation in western Lake Erie. Boxes show interquartile range for each variable, lines within the boxes indicate the median value, and whiskers extend to values ±2 standard deviations from the mean. Units for TSS, VSS, NVSS, and DOC were mg/L, CHL units were μg/L, and CDOM units were in the form of absorption at 400-nm wavelength (m).

Table 2
Single-Variable Regression and Spearman Correlation Analysis Results for PAR Attenuation and Water Quality Parameters

Dependent Variable	Predictor	Model-Adjusted R^2	Model RMSE	Correlation Coefficient	Correlation p Value
$k_{d(PAR)}$	CHL	0.03	1.28	0.32	0.16
$k_{d(PAR)}$	VSS	0.09	1.24	0.52	0.06
$k_{d(PAR)}$	DOC	0.13	1.21	0.62	<0.01*
$k_{d(PAR)}$	CDOM	0.13	1.21	0.60	<0.01*
$k_{d(PAR)}$	NVSS	0.81	0.56	0.83	<0.01*
$k_{d(PAR)}$	TSS	0.85	0.51	0.85	<0.01*

Note. Asterisk signifies statistical significance at $p = 0.05$.

especially true considering the potential impacts of cyanobacterial blooms and agriculturally dominated tributary loads that are often largely confined to the southern half of the western basin, while the relatively transparent waters of the Detroit River influence the northern half of the western basin (Figure 1). Turbidity and primary production conditions within Lake Erie have changed over time, and show a high degree of variability, even over short time periods (Binding et al., 2015; Dahl et al., 1995; Porta et al., 2005). Lake-wide and nearshore water clarity in Lake Erie has generally increased between 1998 and 2014, despite year-to-year variability, while wind and storm events can influence sediment resuspension and turbidity on a day-to-day and seasonal scale. Primary production also showed an increase between 2002 and 2003 (Porta et al., 2005), coinciding with increases in both chlorophyll *a* concentration and PAR attenuation coefficient and a potential decrease in water clarity (Binding et al., 2015). It is possible that $k_{d(PAR)}$ differences between studies can be attributed to the changing primary productivity, water clarity, and resuspension conditions within the western basin. In comparison to other water bodies, the attenuation coefficients fall within a similar range of values as the lower and middle basins of Ireland's Shannon Estuary (McMahon et al., 1992), but were found to be roughly twice as high as those observed in Delaware Estuary (Wang et al., 1996).

The western basin of Lake Erie can be described as an example of case II water (Mobley et al., 2004; Morel & Prieur, 1977; Twardowski et al., 2001)—shallow, coastal zone water for which light attenuation is generally governed by suspended mineral solids in the water. The models' dependence on TSS and NVSS in predicting PAR attenuation (Spearman's $\rho = 0.85$ and 0.83, respectively) supports this classification. The optimal model, as determined by a stepwise regression of $k_{d(PAR)}$ against TSS, VSS, NVSS, DOC, CDOM, and CHL, incorporated NVSS, DOC, and CHL (AIC = −342.02, RSS = 33.33; Table S2), as well as an error term (ε). This model (equation (2), above) explains 89.7% of the variability in the $k_{d(PAR)}$ data across western Lake Erie. Residuals indicate that PAR attenuation is slightly overpredicted by the model at low values of $k_{d(PAR)}$ and underpredicted at high values (Figure 8). This has been observed in previous analyses (Xu et al., 2005), and may reflect some nonlinearity in the influence of suspended mineral particles on scattering and attenuation, resulting from variables such as particle size, shape, and composition that may influence light scattering but are not reflected in a gravimetric measurement of concentration.

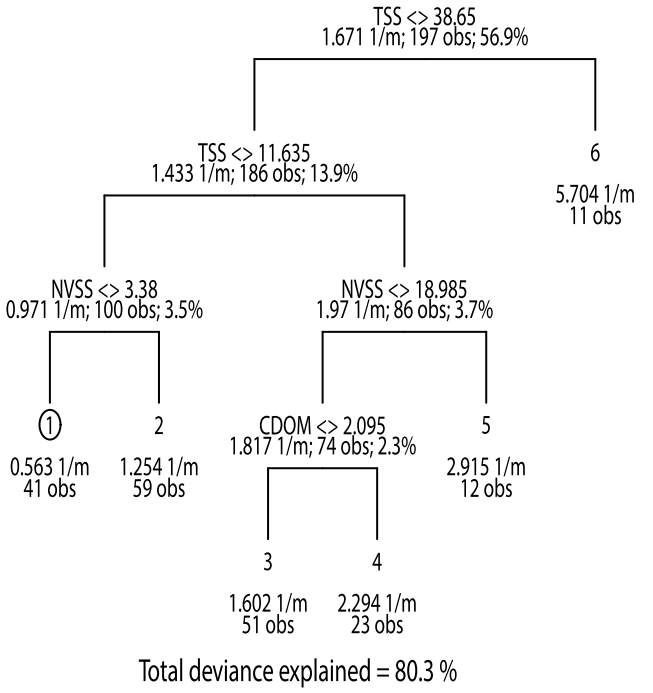

Figure 6. Regression tree analysis results showing relative influence of TSS, VSS, NVSS, DOC, CDOM, and CHL on $k_{d(PAR)}$, showing significant impacts of TSS, NVSS, and CDOM.

The results of the multiple regression models developed here are similar to results from previous model development for natural waters, in both predictive capacity and significant predictor variables. Devlin et al. (2009) modeled $k_{d(PAR)}$ in coastal and transitional marine waters surrounding the UK using the Beer–Lambert law and lognormal, linear, and gamma generalized linear models to predict $k_{d(PAR)}$. Similar models for $k_{d(PAR)}$ were developed for coastal waters in the Mediterranean Sea, English Channel, and Atlantic Ocean by Saulquin et al. (2013). These diffuse attenuation models yielded comparable predictive ability to those for western Lake Erie, explaining 76–99% of the variation in their respective data. Models from Devlin and Saulquin included CHL, CDOM, and suspended particulate matter as significant correlates with $k_{d(PAR)}$; these predictors align with those for western Lake Erie $k_{d(PAR)}$, indicating that PAR attenuation depends on particulate matter, CDOM, and CHL concentrations, across locations. Single-variable regression analyses indicate that minerogenic suspended solids (NVSS) have the greatest impact on PAR attenuation, compared to the five other predictors. This supports the previous findings of Smith (1982) in northwest Africa, Xu et al. (2005) in Chesapeake Bay, and Swain (1980) and Stefan et al. (1983) for Lake Chicot in Arkansas.

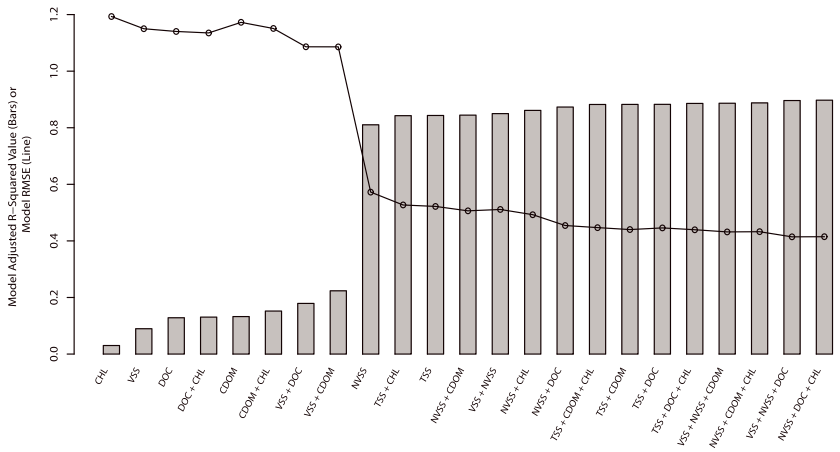

Figure 7. Performance ranking of linear regression models for $k_{d(PAR)}$. Models were ranked by adjusted *R*-squared (bars) and 10-fold cross-validation RMSE (line) values.

Comparisons of specific fitted predictor values between the multiple regression models developed herein and those in previous work show high degrees of variability. The fitted values for suspended solids developed here are larger in magnitude than those from the literature. Relative to those fitted parameters for the similarly shallow and turbid lower basin of Lake Chicot from Stefan et al. (1983), the present models yield fitted suspended solids values 13.9–55.4% larger in magnitude. Likewise, the model herein produces a fitted TSS value that is 22.4% higher than that produced for Chesapeake Bay by Xu et al. (2005). The fitted CDOM parameter for our model is 58% lower than that for a similar model for estuaries in the northeastern United States (Branco & Kremer, 2005), though they fall in the same range ($0.05 < \text{CDOM} < 0.5$ m) as fixed CDOM values that maximize correct prediction of $k_{d(\text{PAR})}$ in the Baltic Sea (Pierson et al., 2008). The variation between fitted parameters could be attributed to the inherent variability in CDOM between water bodies due to terrestrial inputs, mixing processes, and differences between freshwater and estuarine coastal environments. The differences may also be associated with slight differences in the metric used for CDOM characterization: Branco and Kremer (2005) presented a model of $k_{d(\text{PAR})}$ using CDOM absorbance at 350-nm wavelength, while the present models and those used in Pierson et al. (2008) utilized CDOM absorbance at 400 nm.

Interestingly, the comparison of CHL fitted values shows an opposite trend, with the fitted single-variable CHL value for the present model 80.0% lower in magnitude than that developed for Lake Chicot (Stefan et al., 1983). This is likely a function of the very small fitted parameter values for CHL in western Lake Erie. In

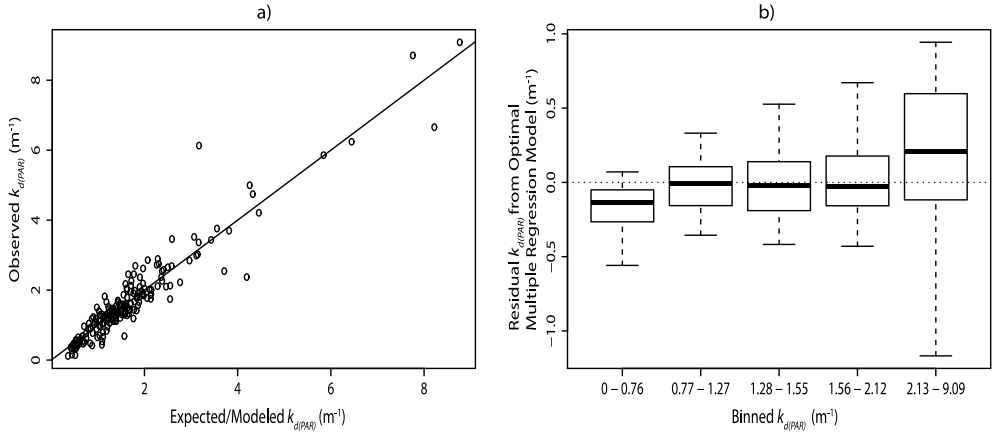

Figure 8. (a) Observed versus model-predicted $k_{d(PAR)}$ values. (b) Residual boxplots binned by $k_{d(PAR)}$ level, binned into five groups of equal sample size and increasing $k_{d(PAR)}$. Both plots show that the model slightly overpredicts at low $k_{d(PAR)}$ and underpredicts at high $k_{d(PAR)}$.

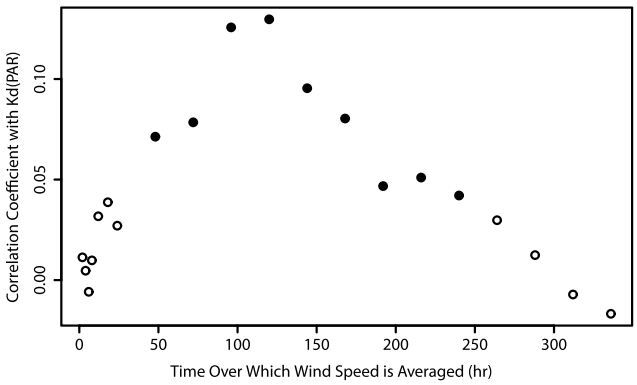

Figure 9. Correlation coefficients for PAR attenuation and wind speed averaged over 2–336 hr; filled circles represent significant correlations (at $\alpha = 0.05$), while open circles denote nonsignificant correlations. In all cases, water depth was an additional predictor variable.

Lake Chicot, fitted CHL values are always positive, while they can be positive or negative for western Lake Erie, reinforcing differences in the impacts of CHL on PAR attenuation between water bodies and basins.

PAR attenuation is a function of absorption and scattering, but it can be impacted by particle size, shape, or color within the water. The Beer–Lambert model does not account for these inherent particle characteristics, instead relying solely on particle mass concentration and perhaps overlooking local and regional effects on inherent optical properties. Further, impacts of one predictor may be transferred to other, cross-correlated predictor variables. Because the inherent optical properties of the particle mass concentration and cross correlations between variables can vary across systems (Kirk, 1984; Siegel et al., 2005; Stramski et al., 2001), the dependence of these models solely on mass concentration is also not constant between systems. Therefore, the lack of local effects within the Beer–Lambert and multiple regression models can be a limitation.

Water quality variables representing minerogenic particles, organic particles, and chromophoric dissolved organic matter, respectively, were interchangeable within the models without sacrificing predictive power. For instance, a model utilizing VSS, NVSS, and DOC had an adjusted R^2 value 0.001 lower, an RMSE 0.003 higher, and an RSS 0.4 higher than a model incorporating NVSS, DOC, and CHL. Models interchanging TSS and NVSS or DOC and CDOM resulted in differences in R^2 and RMSE on the order of 0.01, and differences in RSS ranging from 0.1 to 3.0. As a result of these small differences in skill statistics, these models are accessible to researchers with a wide variety of available empirical water quality data.

Negative intercepts observed in 5 of the 23 multiple regression models indicate that these models may produce unrealistic values of $k_{d(\mathrm{PAR})}$ in water with lower concentrations of scattering and absorbing constituents than in our data. The majority of the negative intercepts determined by our models were not significantly different from zero, though three models with high predictive capability yielded statistically significant, negative intercepts. Incorporating a fixed positive intercept that represents a PAR attenuation coefficient for pure water is an approach sometimes used (e.g., Buiteveld, 1995; Smith & Baker, 1978). However, $k_{d(\mathrm{PAR})}$ for pure water is not a constant, but rather depends on euphotic zone depth and other variables (Gordon, 1989; Morel, 1988; Pegau et al., 1997; Saulquin et al., 2013) and may not be necessary for turbid, case II waters such as western Lake Erie.

In shallow case II waters, wind speed has a large impact on water movement and wave energy, leading to sediment resuspension and increased PAR attenuation. Thus, we evaluated prediction of $k_{d(\mathrm{PAR})}$ using physical variables alone. Models using water depth and 120- or 144-hr averaged wind speed explained the highest proportion of variance in the data. The observation that 120-hr (five-day) average wind speed was the most predictive time-averaged wind speed provides some insight into the time required for particles in the lake to settle after resuspension associated with a wind event. However, wind speed alone explained only a small fraction of the variance in $k_{d(\mathrm{PAR})}$ relative to water quality variables, so further examination of physical predictors of PAR attenuation is warranted.

5. Conclusions

The Beer–Lambert model of exponential decay of light with water depth was found to approximate PAR attenuation in the shallow, turbid waters of western Lake Erie well, with 96% of models capturing over 90% of the variability in PAR data over the water column. Even so, standardized residuals were greater than 1 for some depths, indicating some systematic error in the Beer–Lambert model. Such systematic error was likely associated with mechanisms not represented by the model, such as the varying attenuation of individual wavelengths of light across the PAR spectrum.

Light attenuation in natural waters is a result of scattering and absorption by inorganic particles, organic particles, and dissolved substances. Water quality variables representing these three categories were reliable predictors of $k_{d(\mathrm{PAR})}$ in western Lake Erie. Inorganic particles had the greatest impact on $k_{d(\mathrm{PAR})}$, with dissolved

organic matter having an intermediate impact, and organic particles had the least influence on PAR attenuation. Single-variable models explained up to 84% of the variance in $k_{d(\mathrm{PAR})}$, but combining predictor variables increased model predictive skill. Nine multiple regression models explained 87.3–89.8% of the variability in the $k_{d(\mathrm{PAR})}$ data and showed similar skill in prediction outside of the training data set (cross-validation RMSE range: 0.41–0.46 m). Thus, several different combinations of predictor variables may be used to predict $k_{d(\mathrm{PAR})}$ with similar skill.

Acknowledgments
This study was partially supported through funding awarded to NOAA under the U.S. EPA Great Lakes Restoration Initiative program and awarded to the University of Michigan under the NOAA Cooperative Agreement award NA17OAR4320152. This publication is contribution 1132 for the Cooperative Institute for Great Lakes Research and contribution 1895 for the NOAA Great Lakes Environmental Research Lab. Additional funding and support were provided through the Cooperative Institute for Great Lakes Research (CIGLR) Great Lakes Summer Fellows Program. Data used in analysis can be obtained from the supporting information accompanying this text).

References

APHA (1998). *Standard Methods for the Examination of Water and Wastewater*. Washington, DC: American Public Health Association.
Beletsky, D., Schwab, D. J., Roebber, P. J., McCormick, M. J., Miller, G. S., & Saylor, J. H. (2003). Modeling wind-driven circulation during the March 1998 sediment resuspension event in Lake Michigan. *Journal of Geophysical Research*, *108*(C2), 3038. https://doi.org/10.1029/2001JC001159
Binding, C. E., Greenberg, T. A., Watson, S. B., Rastin, S., & Gould, J. (2015). Long term water clarity changes in North America's Great Lakes from multi-sensor satellite observations. *Limnology and Oceanography*, *16*, 1976–1995.
Bocaniov, S. A., Leon, L. F., Rao, Y. R., Schwab, D. J., & Scavia, D. (2016). Simulating the effect of nutrient reduction on hypoxia in a large lake (Lake Erie, USA-Canada) with a three-dimensional lake model. *Journal of Great Lakes Research*, *42*(6), 1228–1240. https://doi.org/10.1016/j.jglr.2016.06.001
Borsuk, M. E., & Stow, C. A. (2000). Bayesian parameter estimation in a mixed-order model of BOD decay. *Water Research*, *34*(6), 1830–1836. https://doi.org/10.1016/S0043-1354(99)00346-2
Branco, A. B., & Kremer, J. N. (2005). The relative importance of chlorophyll and colored dissolved organic matter (CDOM) to the prediction of the diffuse attenuation coefficient in shallow estuaries. *Estuaries*, *28*(5), 643–652. https://doi.org/10.1007/BF02732903
Buiteveld, H. (1995). A model for calculation of diffuse light attenuation (PAR) and Secchi depth. *Netherlands Journal of Aquatic Ecology*, *29*(1), 55–65. https://doi.org/10.1007/BF02061789
Cerco, C. F., & Meyers, M. (2000). Tributary refinements to Chesapeake Bay model. *Journal of Environmental Engineering-Asce*, *126*(2), 164–174. https://doi.org/10.1061/(ASCE)0733-9372(2000)126:2(164)
Chandler, D. C. (1942). Limnological studies of western Lake Erie II. Light penetration and its relation to turbidity. *Ecology*, *23*(1), 41–52. https://doi.org/10.2307/1930871
Chen, C. S., Liu, H. D., & Beardsley, R. C. (2003). An unstructured grid, finite-volume, three-dimensional, primitive equations ocean model: Application to coastal ocean and estuaries. *Journal of Atmospheric and Oceanic Technology*, *20*(1), 159–186. https://doi.org/10.1175/1520-0426(2003)020<0159:AUGFVT>2.0.CO;2
Christian, D., & Sheng, Y. P. (2003). Relative influence of various water quality parameters on light attenuation in Indian River lagoon. *Estuarine, Coastal and Shelf Science*, *57*(5–6), 961–971. https://doi.org/10.1016/S0272-7714(03)00002-7
Dahl, J. A., Graham, D. M., Dermott, R., Johannsson, O. E., Millard, E. S., & Myles, D. D. (1995). Lake Erie 1993, western, west central and eastern basins: Change in trophic status, and assessment of the abundance, biomass and production of the lower trophic levels. *Canadian Technical Report of Fisheries and Aquatic Sciences*, *2070*(i-xii), 1–118.
Dennison, W. C., Orth, R. J., Moore, K. A., Stevenson, J. C., Carter, V., Kollar, S., Bergstrom, P. W., et al. (1993). Assessing water-quality with submersed aquatic vegetation. *Bioscience*, *43*(2), 86–94. https://doi.org/10.2307/1311969
Devlin, M. J., Barry, J., Mills, D. K., Gowen, R. J., Foden, J., Sivyer, D., Greenwood, N., et al. (2009). Estimating the diffuse attenuation coefficient from optically active constituents in UK marine waters. *Estuarine, Coastal and Shelf Science*, *82*(1), 73–83. https://doi.org/10.1016/j.ecss.2008.12.015
Ensor, D. S., & Pilat, M. J. (1971). Effect of particle size distribution on light transmittance measurement. *American Industrial Hygiene Association Journal*, *32*(5), 287–292. https://doi.org/10.1080/0002889718506462
Fitzpatrick, M. A. J., Munawar, M., Leach, J. H., & Haffner, G. D. (2007). Factors regulating primary production and phytoplankton dynamics in western Lake Erie. *Fundamental and Applied Limnology*, *169*(2), 137–152. https://doi.org/10.1127/1863-9135/2007/0169-0137
Ge, Z. F., Whitman, R. L., Nevers, M. B., Phanikumar, M. S., & Byappanahalli, M. N. (2012). Nearshore hydrodynamics as loading and forcing factors for *Escherichia coli* contamination at an embayed beach. *Limnology and Oceanography*, *57*(1), 362–381. https://doi.org/10.4319/lo.2012.57.1.0362
Gordon, H. R. (1989). Can the Lambert-Beer law be applied to the diffuse attenuation coefficient of ocean water? *Limnology and Oceanography*, *34*(8), 1389–1409. https://doi.org/10.4319/lo.1989.34.8.1389
Gordon, H. R., & McCluney, W. R. (1975). Estimation of depth of sunlight penetration in sea for remote-sensing. *Applied Optics*, *14*(2), 413–416. https://doi.org/10.1364/AO.14.000413
Hondzo, M., & Stefan, H. G. (1993). Lake water temperature simulation-model. *Journal of Hydraulic Engineering*, *119*(11), 1251–1273. https://doi.org/10.1061/(ASCE)0733-9429(1993)119:11(1251)
Houser, J. N. (2006). Water color affects the stratification, surface temperature, heat content, and mean epilimnetic irradiance of small lakes. *Canadian Journal of Fisheries and Aquatic Sciences*, *63*(11), 2447–2455. https://doi.org/10.1139/f06-131
Hutchinson, G. E., & Edmondson, Y. H. (1957). *A Treatise on Limnology*. New York: Wiley, University of California.
Ingle, J. D., & Crouch, S. R. (1988). *Spectrochemical Analysis*. Prentice Hall, NJ. Englewood Cliffs.
Jerlov, N. G. (1968). *Optical Oceanography*. Amsterdam: Elsevier Publishing Company.
Ji, R. B., Davis, C., Chen, C. S., & Beardsley, R. (2008). Influence of local and external processes on the annual nitrogen cycle and primary productivity on Georges Bank: A 3-D biological-physical modeling study. *Journal of Marine Systems*, *73*(1–2), 31–47. https://doi.org/10.1016/j.jmarsys.2007.08.002
Karlsson, J., Bystrom, P., Ask, J., Ask, P., Persson, L., & Jansson, M. (2009). Light limitation of nutrient-poor lake ecosystems. *Nature*, *460*(7254), 506–509. https://doi.org/10.1038/nature08179
Kemp, W. M., Boynton, W. R., Adolf, J. E., Boesch, D. F., Boicourt, W. C., Brush, G., Cornwell, J. C., et al. (2005). Eutrophication of Chesapeake Bay: Historical trends and ecological interactions. *Marine Ecology Progress Series*, *303*, 1–29. https://doi.org/10.3354/meps303001
Kirk, J. T. O. (1983). *Light and Photosynthesis in Aquatic Ecosystems* (Vol. i-xi, pp. 1–401). Cambridge: Cambridge University Press.
Kirk, J. T. O. (1984). Dependence of relationship between inherent and apparent optical properties of water on solar altitude. *Limnology and Oceanography*, *29*(2), 350–356. https://doi.org/10.4319/lo.1984.29.2.0350

Markager, S., & Vincent, W. F. (2000). Spectral light attenuation and the absorption of UV and blue light in natural waters. *Limnology and Oceanography*, *45*(3), 642–650. https://doi.org/10.4319/lo.2000.45.3.0642

McMahon, T. G., Raine, R. C. T., Fast, T., Kies, L., & Patching, J. W. (1992). Phytoplankton biomass, light attenuation and mixing in the Shannon estuary, Ireland. *Journal of the Marine Biological Association of the United Kingdom*, *72*(03), 709–720. https://doi.org/10.1017/S0025315400059464

Medrano, E. A., Uittenbogaard, R. E., Pires, L. M. D., van de Wiel, B. J. H., & Clercx, H. J. H. (2013). Coupling hydrodynamics and buoyancy regulation in *Microcystis aeruginosa* for its vertical distribution in lakes. *Ecological Modelling*, *248*, 41–56. https://doi.org/10.1016/j.ecolmodel.2012.08.029

Mitchell, B. G., Kahru, M., Wieland, J., & Stramska, M. (2003). In J. L. Mueller, G. S. Fargion, & C. R. McClain (Eds.), *Ocean Optics Protocols of Satellite Ocean Color Sensor Validation* (pp. 39–64). Greenbelt, MD, USA: NASA.

Mobley, C. D., Stramski, D., Bissett, W. P., & Boss, E. (2004). Optical modeling of ocean water: Is the case 1-case 2 classification still useful? *Oceanography*, *17*(2), 61–67.

Morel, A. (1988). Optical modeling of the upper ocean in relation to its biogenous matter content (case I waters). *Journal of Geophysical Research*, *93*(C9), 10,749–10,768. https://doi.org/10.1029/JC093iC09p10749

Morel, A., & Prieur, L. (1977). Analysis of variations in ocean color. *Limnology and Oceanography*, *22*(4), 709–722. https://doi.org/10.4319/lo.1977.22.4.0709

Mortimer, C. H. (1987). 50 years of physical investigations and related limnological studies on Lake Erie, 1928–1977. *Journal of Great Lakes Research*, *13*(4), 407–435. https://doi.org/10.1016/S0380-1330(87)71664-5

Mouw, C., & Barnett, A. (2014). *CDOM Absorption—Sample Collection and Analysis* (pp. 1–9). MI: Michigan Technological University Houghton.

Paulson, C. A., & Simpson, J. J. (1977). Irradiance measurements in upper ocean. *Journal of Physical Oceanography*, *7*(6), 952–956. https://doi.org/10.1175/1520-0485(1977)007<0952:IMITUO>2.0.CO;2

Pegau, W. S., Gray, D., & Zaneveld, J. R. V. (1997). Absorption and attenuation of visible and near-infrared light in water: Dependence on temperature and salinity. *Applied Optics*, *36*(24), 6035–6046. https://doi.org/10.1364/AO.36.006035

Pierson, D. C., Kratzer, S., Strombeck, N., & Hakansson, B. (2008). Relationship between the attenuation of downwelling irradiance at 490 nm with the attenuation of PAR (400 nm–700 nm) in the Baltic Sea. *Remote Sensing of Environment*, *112*(3), 668–680. https://doi.org/10.1016/j.rse.2007.06.009

Porta, D., Fitzpatrick, M. A. J., & Haffner, G. D. (2005). Annual variability of phytoplankton primary production in the western basin of Lake Erie (2002–2003). *Journal of Great Lakes Research*, *31*, 63–71. https://doi.org/10.1016/S0380-1330(05)70305-1

Rowe, M. D., Anderson, E. J., Vanderploeg, H. A., Pothoven, S. A., Elgin, A. K., Wang, J., & Yousef, F. (2017). Influence of invasive quagga mussels, phosphorus loads, and climate on spatial and temporal patterns of productivity in Lake Michigan: A biophysical modeling study. *Limnology and Oceanography*, *62*(6), 2629–2649. https://doi.org/10.1002/lno.10595

Rowe, M. D., Anderson, E. J., Wynne, T. T., Stumpf, R. P., Fanslow, D. L., Kijanka, K., Vanderploeg, H. A., et al. (2016). Vertical distribution of buoyant *Microcystis* blooms in a Lagrangian particle tracking model for short-term forecasts in Lake Erie. *Journal of Geophysical Research: Oceans*, *121*, 5296–5314. https://doi.org/10.1002/2016JC011720

Safaie, A., Wendzel, A., Ge, Z. F., Nevers, M. B., Whitman, R. L., Corsi, S. R., & Phanikumar, M. S. (2016). Comparative evaluation of statistical and mechanistic models of *Escherichia coli* at beaches in southern Lake Michigan. *Environmental Science & Technology*, *50*(5), 2442–2449. https://doi.org/10.1021/acs.est.5b05378

Saulquin, B., Hamdi, A., Gohin, F., Populus, J., Mangin, A., & d'Andon, O. F. (2013). Estimation of the diffuse attenuation coefficient K-dPAR using MERIS and application to seabed habitat mapping. *Remote Sensing of Environment*, *128*, 224–233. https://doi.org/10.1016/j.rse.2012.10.002

Siegel, D. A., Maritorena, S., Nelson, N. B., & Behrenfeld, M. J. (2005). Independence and interdependencies among global ocean color properties: Reassessing the bio-optical assumption. *Journal of Geophysical Research*, *110*, C07011. https://doi.org/10.1029/2004JC002527

Smith, R. C., & Baker, K. S. (1978). Optical classification of natural waters. *Limnology and Oceanography*, *23*(2), 260–267. https://doi.org/10.4319/lo.1978.23.2.0260

Smith, R. E. H., Hiriart-Baer, V. P., Higgins, S. N., Guildford, S. J., & Charlton, M. N. (2005). Planktonic primary production in the offshore waters of dreissenid-infested Lake Erie in 1997. *Journal of Great Lakes Research*, *31*, 50–62. https://doi.org/10.1016/S0380-1330(05)70304-X

Smith, W. O. (1982). The relative importance of chlorophyll, dissolved and particulate material, and seawater to the vertical extinction of light. *Estuarine, Coastal and Shelf Science*, *15*(4), 459–465. https://doi.org/10.1016/0272-7714(82)90054-3

Speziale, B. J., Schreiner, S. P., Giammatteo, P. A., & Schindler, J. E. (1984). Comparison of N,N-dimethylformamide, dimethylsulfoxide, and acetone for extraction of phytoplankton chlorophyll. *Canadian Journal of Fisheries and Aquatic Sciences*, *41*(10), 1519–1522. https://doi.org/10.1139/f84-187

Stavn, R. H. (1988). Lambert-Beer law in ocean waters: Optical-properties of water and of dissolved/suspended material, optical energy budgets. *Applied Optics*, *27*(2), 222–231. https://doi.org/10.1364/AO.27.000222

Stefan, H. G., Cardoni, J. J., Schiebe, F. R., & Cooper, C. M. (1983). Model of light penetration in a turbid lake. *Water Resources Research*, *19*(1), 109–120. https://doi.org/10.1029/WR019i001p00109

Stramski, D., Bricaud, A., & Morel, A. (2001). Modeling the inherent optical properties of the ocean based on the detailed composition of the planktonic community. *Applied Optics*, *40*(18), 2929–2945. https://doi.org/10.1364/AO.40.002929

Stumpf, R. P., Wynne, T. T., Baker, D. B., & Fahnenstiel, G. L. (2012). Interannual variability of cyanobacterial blooms in Lake Erie. *PLoS One*, *7*(8), 11.

Swain, A. (1980). Material budgets in Lake Chicot, Arkansas, University of Mississippi, Oxford.

Twardowski, M. S., Boss, E., Macdonald, J. B., Pegau, W. S., Barnard, A. H., & Zaneveld, J. R. V. (2001). A model for estimating bulk refractive index from the optical backscattering ratio and the implications for understanding particle composition in case I and case II waters. *Journal of Geophysical Research*, *106*(C7), 14,129–14,142. https://doi.org/10.1029/2000JC000404

USEPA (2005). Method 415.3: Measurement of total organic carbon, dissolved organic carbon and specific UV absorbance at 254 nm in source water and drinking water. Washington, DC: United States Environmental Protection Agency.

Verhamme, E. M., Redder, T. M., Schlea, D. A., Grush, J., Bratton, J. F., & DePinto, J. V. (2016). Development of the Western Lake Erie ecosystem model (WLEEM): Application to connect phosphorus loads to cyanobacteria biomass. *Journal of Great Lakes Research*, *42*(6), 1193–1205. https://doi.org/10.1016/j.jglr.2016.09.006

Wang, M. Z., Lyzenga, D. R., & Klemas, V. V. (1996). Measurement of optical properties in the Delaware estuary. *Journal of Coastal Research*, *12*(1), 211–228.

Xu, J. T., Hood, R. R., & Chao, S. Y. (2005). A simple empirical optical model for simulating light attenuation variability in a partially mixed estuary. *Estuaries*, *28*(4), 572–580. https://doi.org/10.1007/BF02696068